

Application of a Modified Jogged-Screw Model for Creep of TiAl and α -Ti Alloys

G.B. VISWANATHAN, S. KARTHIKEYAN, R.W. HAYES, and M.J. MILLS

Stress exponents for creep, in the range of 5, are typically associated with dislocation creep processes, normally associated with a strong tendency for subgrain formation. In this article, we will demonstrate that there are several important alloy systems that have similar stress dependence and, yet, lack this tendency for subgrain formation. Specifically, dislocations in the intermetallic compound γ -TiAl and the hexagonal close-packed (hcp) α phase of the commercial Ti alloy, Ti-6242, tend to be homogeneously distributed with a tendency for alignment along screw orientation. In both alloy systems, the screw dislocations exhibit a large density of pinning points, which detailed transmission electron microscopy (TEM) investigation indicate are locations of tall jogs. These observations suggest that the jogged-screw model for creep should be appropriate after suitable modification for the presence of these tall jogs. This modified jogged-screw (MJS) model is presented, together with a discussion of the assumptions made, and the results of this model are shown to compare favorably with experiment for both alloy systems. The possible criteria for the formation of tall jogs are also described, and the potential application of this modified model to other alloy systems is discussed.

I. INTRODUCTION

A PRIMARY goal of research in the area of high temperature performance of materials is the development of physically-based, microstructure-sensitive, and predictive models of creep deformation. Several classic models for diffusion-mediated creep have been developed by Coble,^[1] Nabarro,^[2] Herring,^[3] and Harper and Dorn.^[4] These models are predictive in that the key physical and microstructural parameters are identified, and the variation of strain rate with temperature and stress appear to agree with experiment under the appropriate deformation conditions and for a variety of materials. The stress dependence of the steady state or minimum creep rate is often used in an attempt to identify the underlying deformation mechanisms for creep. These diffusional-transport models concern conditions of higher temperature and low stresses in which the stress exponents for creep are relatively small (in the range 1 to 2). At higher stresses and lower temperatures, the stress exponents are typically larger, with a value of about 3 for class A solid-solution alloys. Such a power-law exponent is indicative of either a viscous glide mechanism, where dislocations are limited by the rate at which solutes can diffuse with the dislocations,^[5] or a dislocation climb process.^[6] Once again, the foundation of these models is a sound physical picture of the creep process.

The fundamental understanding of creep at higher stresses in pure fcc metals and “class M” alloys, where stress exponents of about 5 are observed, is less satisfactory. Such a

condition has traditionally been associated with “dislocation creep” mechanisms. Weertman^[7] proposed that dislocation production from sources is limited by the climb of dislocations at the tips of dislocation pile-ups. It is principally due to this model that the observation of a stress exponent close to 5 is often taken as proof that creep is controlled by recovery due to dislocation climb. Unfortunately, the physical basis of this model is questionable since dislocation pile-up structures are generally not observed during high temperature creep. In pure metals and class M alloys, it is the development of subgrain structures, with “hard” and “soft” regions, that is thought to be the dominant process.^[8] Thus, modeling of creep in pure metals would appear to require consideration of large numbers of dislocations and their interactions. A new route to modeling 5-power-law creep in subgrain-forming metals is described in a companion article in this volume.^[9]

In this article, we will demonstrate that there are several important alloy systems that appear to have the macroscopic characteristics of a dislocation creep process (*i.e.*, stress exponents of about 5) but, in fact, do not exhibit a strong tendency for subgrain formation. This is the case for creep of the intermetallic compound γ -TiAl and the hexagonal close-packed (hcp) α phase of Ti alloys. Inspired by direct transmission electron microscopy (TEM) observations in these systems, a new model for dislocation creep has been developed^[10] that is based on the classic idea that jogs on screw dislocations may limit high temperature deformation. We will first present, briefly, the conventional jogged-screw model, including its basis and assumptions. Our work to-date has shown that the conventional model is inconsistent with the details of the observed dislocation structures, as well as the measured macroscopic creep behavior. The TEM observations have inspired a modified version of the jogged screw model, which we believe does provide an accurate, physically-based description of creep in γ -TiAl and α -Ti (Al) solid solutions. Indeed, we further expect that this model should be applicable to other hcp solid solutions and possibly to bcc solid solutions as well. We will discuss the dislocation level characteristics that these apparently disparate systems

G.B. VISWANATHAN, Research Scientist, S. KARTHIKEYAN, Graduate Fellow, and M.J. MILLS, Professor, are with the Department of Materials Science and Engineering, The Ohio State University, Columbus, OH 43210. R.W. HAYES is with Metals Technology, Inc., Northridge, CA 91324.

This article is based on a presentation made in the workshop entitled “Mechanisms of Elevated Temperature Plasticity and Fracture,” which was held June 27–29, 2001, in San Diego, CA, concurrent with the 2001 Joint Applied Mechanics and Materials Summer Conference. The workshop was sponsored by Basic Energy Sciences of the United States Department of Energy.

have in common, making them treatable by the same basic model. Since this model provides a link between atomic level processes and macroscopic properties, it represents a natural platform from which to build multiscale treatments of creep deformation in these important materials.

II. THE CONVENTIONAL JOGGED-SCREW MODEL

A classic model for dislocation creep is based on the premise that the steady-state strain rate is determined by the motion of isolated screw dislocations that are nonconservatively dragging jogs.^[11–14] By balancing the work done in translating the gliding portions of the screw dislocation forward against the chemical force required to generate (or consume) the vacancies needed to move the jogs, the basic form for the overall screw velocity is^[15]

$$v_s = (4\pi D/h) \sinh \left\{ \frac{\tau \Omega}{hkT} \right\} \quad [1]$$

where D is the self-diffusion coefficient, Ω is the atomic volume, d is the average spacing between jogs, h is the height of the jogs, and τ is the applied shear stress. The “sinh” functional form results if it is assumed that jogs of the vacancy producing and vacancy absorbing type are present in equal density. Assuming that the mobile screw dislocation density, ρ_s , varies with stress through the Taylor relation,

$$\rho_s = (\tau/\alpha Gb)^2 \quad [2]$$

which has been verified following creep of a number of materials,^[16] then, the jog screw model naturally predicts a stress exponent of 3 at lower stresses, with increasing stress dependence at larger stresses.

It is important to note that in the original developments of this model, it was assumed that the jogs form as a result of the intersection of screw dislocations on different slip systems. This assumption has several implications: (a) the jogs should be of the order of a Burgers vector high, (b) jogs should be seen only under multiple slip conditions, and (c) in a given grain with two operative slip systems, the jogs should all be of the same sign. As discussed in Section III, our detailed TEM studies in γ -TiAl have shown that all three of these assumptions are incorrect, indicating that the jogs actually originate from a source quite different from slip-system intersection.

With the exception of the recent work of Xu and Arsenault^[17] on NiAl, in none of the previous attempts to apply the jogged-screw model has it been shown that jog-dragging screws are actually present following creep deformation. Thus, validation of the model has relied upon comparison with macroscopic creep data.^[11,18] While the functional form predicted by the model can be used to describe creep in a number of materials,^[11,18] the model parameters resulting from these fitting procedures are often beyond their expected range of values.^[11,18] For instance, Barrett and Nix^[11] require a very small jog spacing (21 nm) in order to match experiment. This spacing is far smaller than that observed by Furubayashi *via in situ* TEM experiments^[19] on the same material. He observes an average jog spacing of 170 nm, though it is important to point out that these experiments were done at room temperature. The significant advantage of a physically based model for creep is that the relevant microscopic parameters can be directly measured and verified through TEM observations.

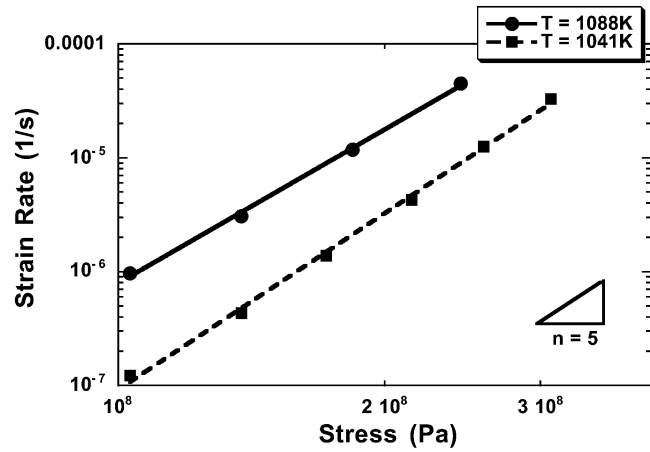


Fig. 1—The log minimum strain rate vs log stress curves for the binary Ti-48Al have been shown for two different temperatures, 1041 and 1088 K.^[20]

We will now present our work on γ -TiAl in which TEM analysis has demonstrated that jogged screw dislocations actually are dominant; however, the conventional jogged-screw model is incapable of predicting the measured creep rates. A new version of the jogged screw model, suitably modified to account for details of the dislocation structure, specifically the presence of *tall jogs*, will then be introduced. This modified jogged-screw (MJS) model appears to provide a reasonably accurate description of creep in this material.

III. DEVELOPMENT OF THE MODIFIED JOGGED-SCREW MODEL

The log-minimum strain rate vs log stress curves for the binary Ti-48Al has been shown in Figure 1 from the work of Viswanathan *et al.*^[20] This material had a nominal composition of Ti-47.86Al-0.116O-0.016N-0.041C-0.076H and was heat treated at 1473 K in the ($\alpha + \gamma$) two-phase region just above the eutectoid temperature and followed by a stabilization treatment at 1173 K for 6 hours. This heat treatment yields a near-gamma microstructure for which the volume fraction of α_2 is small, and γ grains have an equiaxed morphology with a grain size of 50 μm . The creep response in equiaxed γ -TiAl obey a power law in stress, with stress exponents in the range of 5 to 6. Similar results have been widely reported.^[10,21–27]

Thin foils for TEM observations were prepared from discs sectioned normal to the stress axis. The foils of Ti-48Al were thinned using a twin jet electropolisher using a solution consisting of 65 pct ethanol, 30 pct butan-1-ol, and 5 pct perchloric acid, at a voltage of 20 V, current of 30 mA, and temperature of -40°C . Observations on the microstructures were conducted on a PHILIPS* CM200 transmission

*PHILIPS is a trademark of Philips Electronic Instruments Corp., Mahwah, NJ.

electron microscope operated at 200 kV.

The deformation microstructure in the Ti-48Al alloy, at creep strains corresponding with the minimum creep rate, is dominated by $1/2[110]$ -type dislocations. The dislocations tend to be elongated in the screw orientation and appear to be frequently pinned along their lengths, as can be seen in

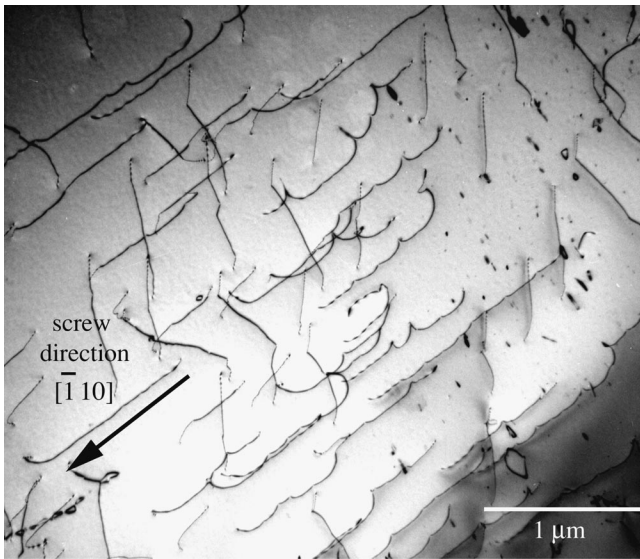


Fig. 2—The deformation microstructure in the Ti-48Al alloy, at creep strains corresponding to the minimum creep rate. Dislocations are $1/2(110)$ type, aligned in the near-screw orientation, and are heavily cusped due to the presence of jogs.

Figure 2. The segments on either side of the pinning points are seen to be bowed out, forming local cusps along the length of the dislocations. The average spacing between the apparent pinning points is around 200 nm. Tilting experiments in the TEM have confirmed that these cusps are frequently associated with jogs on the screw dislocations^[10] and that these jogs are typically much larger than atomic dimensions. The largest jog heights measured at a stress of 210 MPa are about 40 nm. A similar conclusion has been drawn by Sriram *et al.*^[28] based on TEM studies of Ti-52Al following constant strain rate deformation at 573 K. Observations indicate that adjacent jogs typically are of opposite sense (in terms of line direction), meaning that one jog is a step “up” relative to the glide plane, while the adjacent one is a step “down” relative to the glide plane.

The observation of cusped screw segments in the equiaxed structures and the general absence of subgrains (as might be expected for an $n \sim 5$ behavior) suggests that the creep rate may be controlled by the nonconservative motion of jogs along the length of the screw dislocations.^[10] Thus, while the concept of jogged-screw dislocations is clearly applicable to creep of γ -TiAl, the details of the dislocation configurations differ drastically from those assumed in the conventional model, as discussed previously. For instance, these tall jogs may originate not from dislocation intersections but rather as a natural consequence of dislocation motion in γ -TiAl.^[10,29] Jogs may be nucleated intrinsically on screw segments by the collision of two migrating kinks formed on two different glide planes. As the screw segment advances, kinks would tend to collect at these jogs causing them to grow. Subsequent motion of the screw dislocation then requires the nonconservative dragging of these jogs (if lateral, glide motion is difficult).

The presence of tall jogs results in the overall creep rates being much slower than predicted by the conventional jogged-screw model. Jogs taller than a critical height can be assumed to act as a source, rather than being dragged along with the screw dislocation. The oppositely signed,

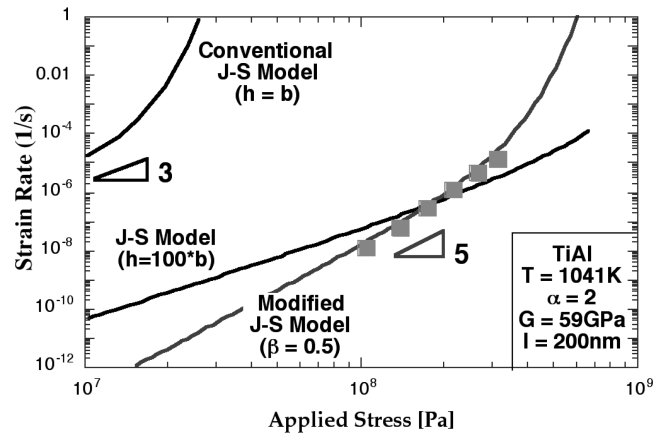


Fig. 3—Predicted axial creep rate vs axial stress using the conventional and modified jogged-screw models, with model parameters appropriate for γ -TiAl. Included for comparison is experimental data from the work of Viswanathan.^[20]

near-edge segments attached to the top and bottom of such a supercritical jog can bypass each other. This critical jog height, h_d is given by

$$h_d = Gb / \{8\pi(1 - \nu)\tau\} \quad [3]$$

If $h > h_d$, then the jog will no longer be dragged by climb but will instead act as a dislocation source. The dislocation source can be envisioned to generate new line length initially having no jogs but rapidly acquires them. In the absence of detailed TEM measurement of jog height distributions with stress or dynamical dislocation calculations to the same end, we now make the assumption that the “characteristic” jog height on a given dislocation segment is a constant fraction of h_d . For the present discussion, we will set the value of h in Eq. [1] equal to βh_d , which yields the following, modified expression for the jogged-screw model:

$$\dot{\gamma} = \left(\frac{\pi \cdot D_s}{\beta \cdot b \cdot h_d} \right) \cdot \left(\frac{\tau}{\alpha \cdot G} \right)^2 \cdot \sinh \left[\frac{\Omega \cdot l \cdot \tau}{4 \cdot \beta \cdot h_d \cdot k \cdot T} \right] \quad [4]$$

In this expression, we have once again assumed that the Taylor relation of Eq. [2] holds.

The predicted axial strain rate as a function of stress using this modified expression is shown in Figure 3 and compared with the creep data of Viswanathan and Vasudevan^[30] for “near-gamma” Ti-48Al. We have assumed a diffusion coefficient of 1.62×10^{-18} m²/s, using the data from Kroll *et al.* for Ti-52Al.^[31] A shear modulus of 59 GPa has been used based on estimates from Reference 32. For the modified model, the value of β is assumed equal to 0.5. Based on direct TEM observations of jog heights, the value of h_d appears to be underestimated using Eq. [3]. This discrepancy could be due to a significant Peierls friction for 60 degree orientations in TiAl,^[33] which will tend to stabilize taller-than-expected jogs. In addition, the near-edge dislocations are not straight and infinitely long but, rather, are bowed. The tallest jogs observed are about four times larger than h_d using Eq. [3], and this factor has been included in the denominator of the sinh function in Eq. [4]. For comparison purposes, the creep rates predicted by the “conventional” jogged-screw model (with the same jog spacing as for the modified model) are also shown assuming that the jogs have a height of $1b$ and $100b$.

As can be clearly seen in Figure 3, the predicted creep rates based on the conventional jogged-screw model and assuming-unit jogs are many orders of magnitude too large when compared to the measured creep rates. If the presence of tall jogs is assumed, except jogs having a *constant* average height (independent of stress), then, the creep rates more closely match those observed. However, the predicted stress exponent of 3 at lower stresses remains significantly smaller than that observed. The incorporation of a *stress-dependent jog height* in the modified model results in a remarkably good agreement between this new model and the experiment. This initial analysis of the modified model would suggest that it is a significant improvement over the conventional jogged-screw model. Furthermore, there are key structural parameters that can be measured to calibrate the model. Thus, the MJS model offers the opportunity of providing a sound, physical picture of the creep process, which is both quantitative and predictive. An extension of the model has also been made to lamellar γ -TiAl, where creep rates are lower, and the stress exponent exhibits two regimes (low exponents (2 to 3) at lower stresses and high exponents (7 to 8) at higher stresses). The predictions of the model, both qualitatively and quantitatively, is quite accurate at high stresses, though further work is required to model the low stress regime for the lamellar case.^[34,35]

Nevertheless, at the present stage in the development of the model, there are several model features, which need to be further discussed and evaluated. These features and their variations with deformation conditions will now be discussed.

Further Discussion of Model Parameters

The key microstructural parameters of the model are the jog spacing, jog height, and dislocation density. The TEM observations indicate that there is indeed a distribution of jog spacings, and a distribution of jog heights is also expected, although this has not yet been measured. In such a case, each jog would move at a different velocity such that the dislocation is no longer oriented in the screw direction. However, microscopic observation does not indicate such dramatically skewed dislocation structures. This leads us to believe that despite the presence of a distribution of jog heights and jog spacings, creep is controlled by certain critical parameters only and that such fluctuations get dissipated quickly, thus, resulting in an "equilibrium" dislocation structure, dictated by these rate-controlling parameters. In Sections III-A-1 and III-A-2, we attempt to discuss some issues related to jog spacing and jog height distributions.

1. Jog spacing

A constant jog spacing of 200 nm has been assumed. The TEM observations of γ -TiAl indicate that the jog spacing has a Gaussian distribution about a mean value, as shown in Figure 4. This result can be argued qualitatively in the following manner (Figure 5):

- (1) In the initial stages on deformation, it may be assumed that unit jogs get nucleated (Figure 5(a)) along the length of the screw dislocation (at a rate dependent on the rate of cross-slip processes). These unit jogs do not offer any significant resistance, and the resulting initial creep rates are high.
- (2) As deformation proceeds, the number of unit jogs

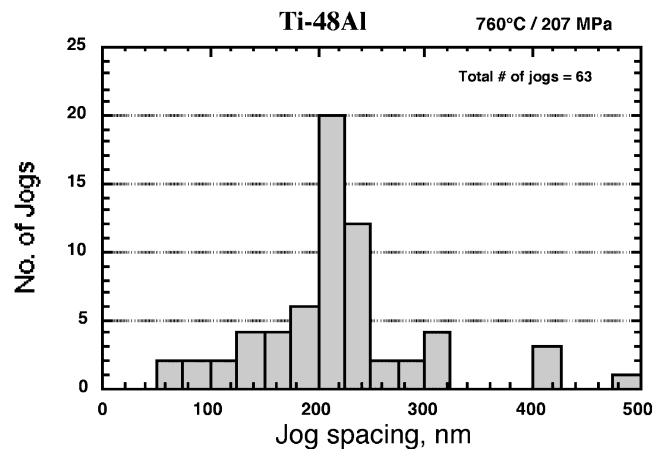


Fig. 4—The distribution of jog spacing. The Orowan spacing is found to be 202 nm, for an applied stress of 207 MPa. This value is indeed very close to the average jog spacing value of 200 nm.

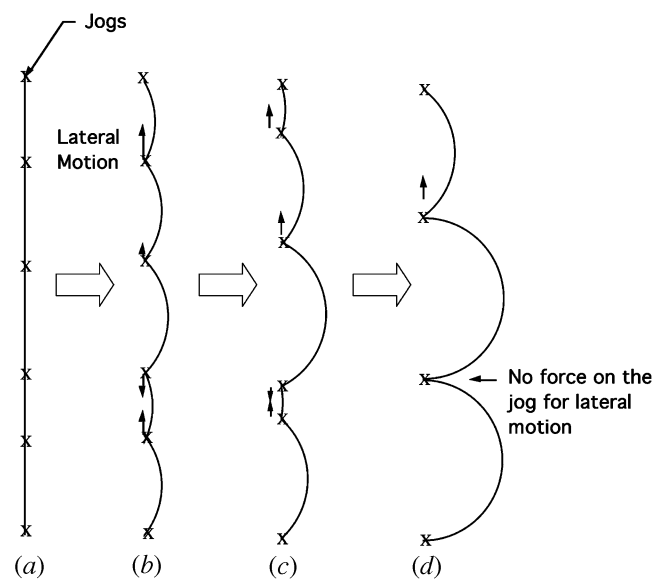


Fig. 5—Schematic showing the sequence of events leading to coarsening of jog spacings: (a) nucleation of jogs, (b) lateral conservative motion of the jogs driven by line tension, (c) closely spaced jogs are driven closer and vice versa, and (d) cusps are symmetrical with minimal lateral forces and, therefore, jog dragging becomes dominant.

increases. As the dislocation segments between neighboring jogs bow out, the jogs experience lateral forces that would tend to move the jog conservatively along the screw direction (Figure 5(b)). Assuming the same curvature for all the bowed-out segments, it is apparent that the lateral force on jogs separated by a smaller spacing will tend to shrink these segments, while jogs that are separated by a larger spacing will tend to become even longer. Lateral conservative motion, driven by line tension, is thus possible when cusps are subcritical.

- (3) These lateral forces will remove very small jog spacings from the distribution. Lateral forces will exist for all jog spacings less than the Orowan spacing (Figures 5(c) and (d)). For spacings greater than this, the lateral movement will be minimal, as the cusps at the jogs are symmetrical in shape. In essence, jog spacings coarsen as closely

spaced jogs are driven closer and *vice versa*. It is presumed that at steady state most of the cusps are symmetrical with minimal lateral forces; therefore, jog dragging becomes dominant.

- (4) The largest jog spacings in the distribution are suppressed by processes where a brand new superjog has nucleated on a particularly long near-screw segment. The probability for such a nucleation event should scale with the distance between existing superjogs, thereby removing the long superjog spacings from the distribution.

Based on this rationale, there should be a tendency toward a Gaussian-like distribution about a mean value. Note that this scenario would suggest that our use of mean jog spacing might be a reasonable approximation. This also suggests that this mean value will be approximately the same as the Orowan spacing (when the cusps are symmetrical). The Orowan spacing is given by

$$l_c = (G \cdot \mathbf{b})/\tau \quad [5]$$

Assuming a nominal stress of 207 MPa, a Schmidt factor of 0.4, G of 59 GPa, and \mathbf{b} of 2.832 Å, we get a Orowan spacing, l_c , of 202 nm. This value is indeed very close to the average value of 200 nm that has been assumed in the model (Figures 3 and 4). However, this also suggests that the mean jog-spacing value would be a function of stress, and this has not been incorporated into the model. Further work needs to be done to confirm these qualitative predictions.

2. Jog height

The maximum jog height, h_d , was approximated in Section III-A using the condition for the breaking of an infinitely long, pure-edge dipole. The measured jog heights are, however, much larger than that predicted by Eq. [3]. This discrepancy may be due to the fact that the near-edge dislocations are not straight and infinitely long but, rather, are bowed. Work needs to be done first to bring a straight jogged-dislocation into a fully bowed configuration where it can behave similar to a dipole and, then, as a source on further increasing the stress. So the maximum jog height may be much larger than that predicted for an infinitely long dipole.

It should be noted that there are three competing processes that can take place at a superjog (Figure 6): (a) jog dragging, (b) dipole extension, and (c) dipole bypass. It is important to know which one of these processes would be most favorable energetically for a jog of a certain height, h . While the former two processes are athermal, jog dragging is not only dependent on the temperature but also on the strain rate. Dragging the jog becomes increasingly favorable with increasing temperature and at smaller strain rates. The minimum stress required for one of the three processes to take place, as a function of the jog height, h , is shown in Figure 7. It is evident from the curve that, under creep conditions (small dislocation velocities), jog dragging is the most favorable process for small jogs, while dipole bypass becomes favorable for jogs taller than a critical limit. However, it is interesting to note that under conditions where the dislocation velocity is large enough to produce high strain rates (for example, under constant strain rate conditions or at lower temperatures) jog dragging is not favorable. Instead, dipole extension should become prevalent. This prediction is consistent with microstructures observed following constant

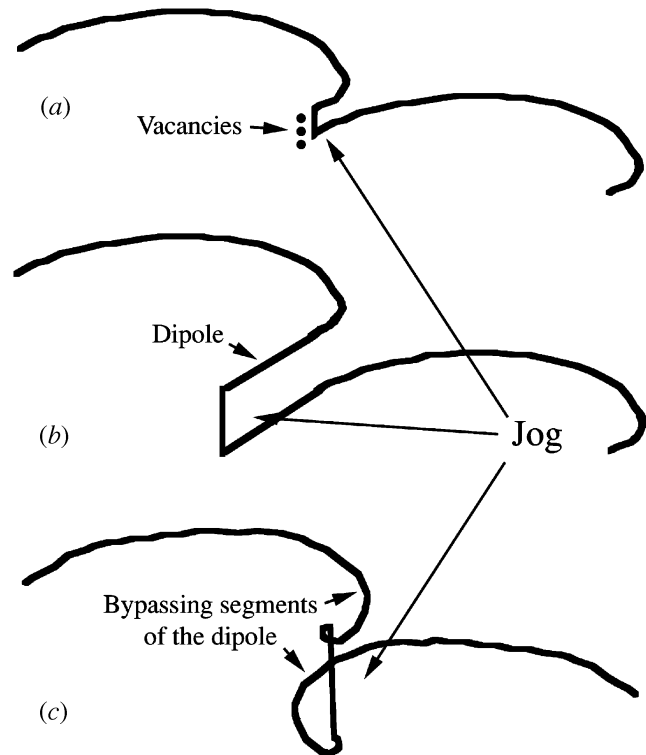


Fig. 6—Schematic indicating the three competing processes that could take place at a jog, under applied shear stress: (a) jog dragging, (b) dipole dragging, and (c) dipole bypass. One of the three processes becomes favorable, depending on the height of the jog, temperature, and dislocation velocity.

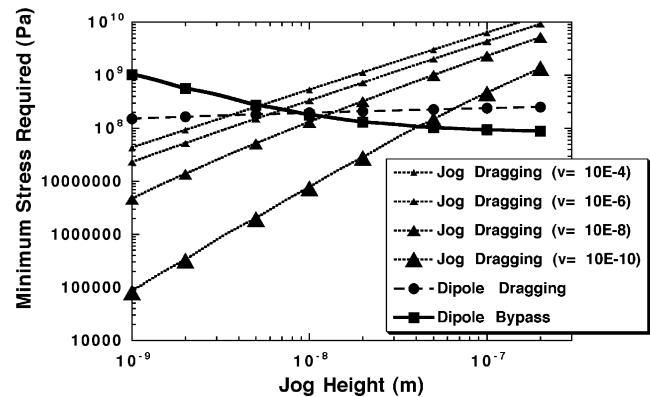


Fig. 7—The plot showing the minimum stress required for initiating one of the three processes, jog dragging, dipole dragging, or dipole bypass, as a function of jog height. The minimum stress for jog dragging has been plotted for different values of dislocation velocity (hence, strain rate). For any given jog height, the process that requires minimum shear stress would be the most dominant.

strain rate testing at 973 K in the same alloy,^[20] as shown in Figure 8.

Based on Figure 6 and assuming that the dislocations indeed move by the nonconservative movement of the jogs along the dislocations, we may predict the critical jog height as a function of stress, as shown in Figure 9. Interestingly, the critical jog height still varies inversely with stress, as we had assumed in Eq. [3]. However, the critical height, thus extracted from Figure 9, is twice that predicted by Eq.

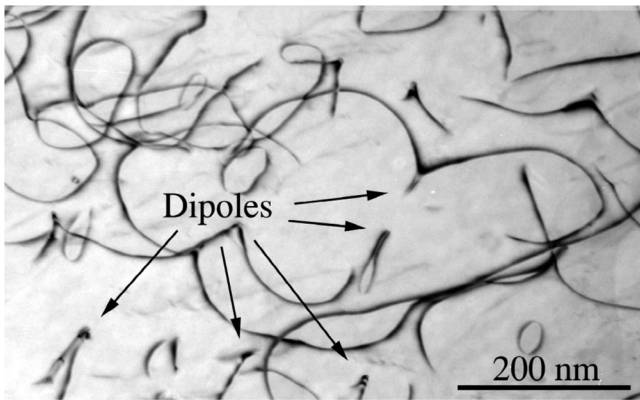


Fig. 8—The TEM micrograph of a Ti-48Al sample tested under tension at a constant strain rate, at 973 K. Note the numerous dipole configurations.

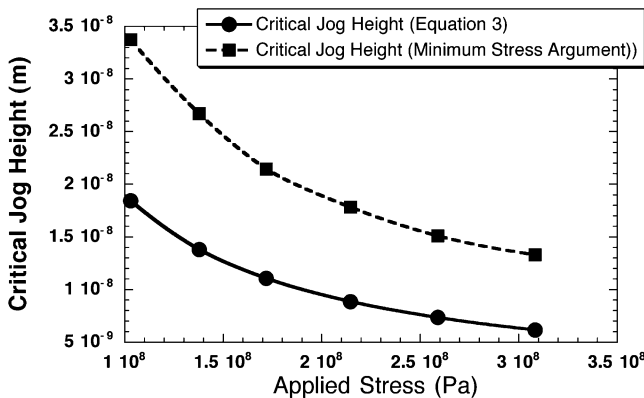


Fig. 9—The critical jog height, above which jogs stop being dragged, is plotted as a function of the applied stress, using Eq. [3] and the “minimum stress” argument. Note that the critical jog height varies inversely with stress in both cases. The minimum stress argument, however, provides a value of critical jog height approximately twice that predicted by Eq. [3].

[3] and in closer agreement with the value deduced from actual jog-height measurements.

A distribution of superjog heights is expected to exist, and we are presently attempting to determine this distribution for several deformation conditions. In the model described previously, we have assumed that, on average, dislocation motion is controlled by dragging of jogs of an average height, half that of the dipole bypass condition. However, the actual dynamics of dislocation motion under these conditions is not simple, and indeed, it is not known presently whether it is the average height of tall jogs or the height of the tallest “draggable” jog (hence, the slowest) that is critical to the process. For instance, the tallest jogs will be pulled more strongly by line tension than will the shorter jogs. Further work needs to be done, through dynamical simulation of dislocation movement, to understand whether it is appropriate to approximate an actual distribution of jog heights with an average quantity, as has been assumed presently.

3. Dislocation density

In adopting the Taylor relationship for the stress-dependence of the dislocation density, we appeal to the fact that this relationship has been found to hold for a variety of materials under creep conditions. It has been found for both class M and class A metals.^[16] The latter case is perhaps

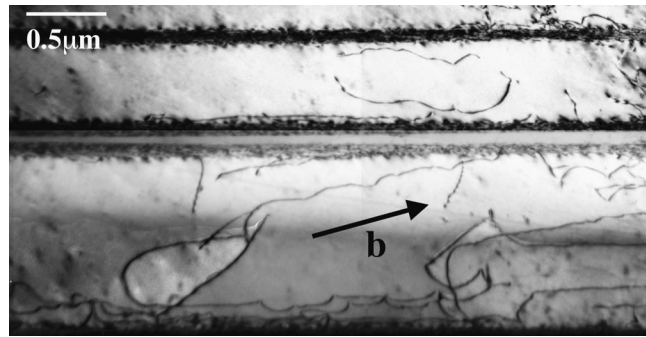


Fig. 10—TEM micrograph of the deformation substructure developed in the α phase of Ti-6242Si. The substructure is dominated by a -type $(1/3\langle 1120 \rangle)$ dislocations that tend to elongate in the screw orientation and are cusped.

most analogous to the present discussion as dislocation mobility is thought to control deformation, as opposed to substructure formation.

IV. EXTENSION OF THE MODIFIED JOGGED-SCREW MODEL TO α -Ti ALLOYS

The preceding discussion demonstrates that the MJS model has validity for understanding creep of γ -TiAl when deformation is dominated by $1/2\langle 110 \rangle$ dislocations. It might initially seem surprising to suggest that a similar model might also be appropriate for creep of α -Ti alloys. These two materials systems clearly have quite different crystal structures and symmetry. However, we will demonstrate a remarkable resemblance in the morphology of the most commonly observed dislocations found after creep in both systems. The fundamental reasons for this similarity in dislocation behavior will also be discussed.

Commercial Ti alloys, used in large quantities for turbine engine applications, are exposed to temperatures in excess of 500 °C for some components. Thus, creep modeling and strategies for creep strengthening are technologically crucial issues in these alloys. Commercial alloys, such as Ti-6242Si, have microstructures with primarily two phases: the hcp α phase and the bcc β phase. The α phase is typically the predominant phase in terms of volume fraction for the “near- α ” alloys. Based on creep work on Ti-6242Si^[36] and on single-phase α alloys,^[37] it is known that the stress exponents lie in the range of 5 to 6. The activation energy for creep is close to that for self-diffusion in α -Ti.^[37] The activation energy for creep is also dependent on impurity content (most notably Ni), based on recent creep measurements by Hayes *et al.*^[38] This variation with Ni is very similar to the effect this impurity has on self-diffusion in α -Ti.^[39] Thus, the stress exponent and activation energy for creep both suggest the “classical” interpretation of dislocation creep controlled by climb recovery. However, the deformation substructure developed during creep suggests that this classical view, in which subgrain formation would be expected, is not valid.

Shown in Figure 10 is a representative TEM micrograph of the deformation substructure developed in the α phase of Ti-6242Si having an α/β colony microstructure in which the α phase represents about 90 pct of the total volume fraction. This specimen was crept to the minimum strain

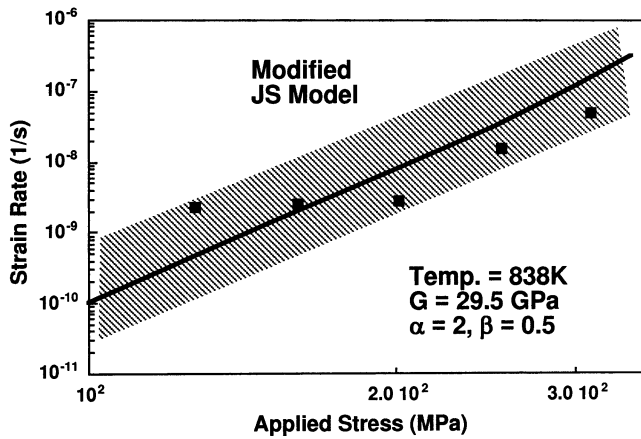


Fig. 11—The observed creep rates in Ti-6242 alloy fall within a range of predicted creep rates (shaded area) using refined MJS model. An average value of the predicted creep rates is displayed.

rate at 310 MPa and 811 K, which corresponds to the “near-five” power-law regime. There is a marked absence of subgrain formation at these strain levels. Instead, the substructure is dominated by a-type $(1/3\langle 11\bar{2}0 \rangle)$ dislocations. While these dislocations tend to elongate in screw orientation, it is remarkable that they also take on cusped configurations very similar to those described previously for the ordered γ phase of TiAl. Tilting experiments have further demonstrated that these cusps often correspond to tall jogs that link bowed segments that are gliding on either basal or prism glide planes.

The screw orientation is strongly favored for a-type dislocations at lower temperatures. Bond-order calculations by Gershick *et al.*^[40] for the a-type screw dislocation in pure Ti indicate that the screw component should be spread simultaneously in both basal and prism planes. The cores are nonetheless very compact; so cross-slip should be quite prevalent. Indeed, it is well known that the screw orientation is strongly favored during deformation at lower temperatures.^[41] Finally, these alloys typically contain alloying additions that provide solute strengthening, leading to strong interaction with dislocations of edge character and more sluggish lateral expansion of kink- and jog-pairs. Thus, conditions are indeed favorable for superjog formation along a-type dislocations.

We have attempted to apply the MJS model to predict the creep response of lamellar Ti-6242 in a manner similar to that described previously for γ -TiAl. We have once again assumed that the jog spacing is invariant with stress and that we may model the superjogs with a characteristic jog height. Based on TEM observations, the upper-bound jog height, h_d , is about 4.3 nm, and we have again assumed a value of 0.5 for β . In a further extension of this model, the lath morphology of the α -phase bounded on either side by β laths has been incorporated. As detailed elsewhere,^[38] this refined model allows different strain rate predictions depending on the operative a-type slip system, and whether dislocation motion is occurring on basal or prism planes.^[38] Figure 11 shows that the observed creep rates in Ti-6242 fall within a range of predicted creep rates (shaded area) using the MJS model and an average value of the predicted strain rates is displayed. Silicide precipitation also occurs that during the course of creep deformation (as a result

of β -phase dissolution). Strong interaction between these silicides and a-type dislocations are observed, indicating that many of the dislocations included in our density measurements may not be free to participate in creep deformation and could negatively affect the creep rates. In addition, a distinct change in stress exponent is seen in the experimental data at low stress, which is not consistent with the MJS model. This transition may reflect a change in creep mechanism at low stresses. Nevertheless, the model reasonably reproduces the observed stress dependence at higher stresses.

A more direct comparison between the MJS model and experiment would be offered by creep studies and substructure characterization of a single α -phase alloy, such as Ti-6 wt pct Al, in which the complications due to the presence of β phase and silicide precipitates present in Ti-6242Si may be avoided.

V. POSSIBLE EXTENSION TO OTHER SYSTEMS

Based upon the earlier ideas of Ikeno and Furubayashi,^[42] and later by Louchet and Viguier,^[29] we may summarize the conditions required for the “natural” development of superjogs on screws as the following.

- (a) Screws are compact such that cross-slip is relatively easy.
- (b) Screw orientation is favored due to strong lattice friction.
- (c) Jog-pair and kink-pair expansion is sluggish due to lattice or solute friction.

Criteria (a) and (b) ensure that cross-slip events are frequent and that there are long lengths of dislocations in screw orientation, thereby increasing the probability of forming superjogs. If kink-pair and jog-pair expansion is very rapid (relative to their rate of creation), then superjog creation is less likely, which accounts for criterion (c).

The bcc solid solutions are, therefore, likely candidates for superjog formation. The preferential alignment of dislocations along screw orientation at lower temperatures in bcc metals has been attributed to a nonplanar, three-fold spreading of the $1/2\langle 111 \rangle$ dislocation core on $\{112\}$ or $\{110\}$ planes.^[43] The spreading is small and cross slip is common.^[42] Thus, the requirements for superjog formation are present. *In situ* TEM observations in pure Nb^[42,44,45] and postmortem observations in Fe-3 pct Si^[19,46] indicate that superjogs are frequently formed. It is, therefore, postulated that the MJS model may be applicable for this broad class of alloys. The requirement that kink-pairs not expand very rapidly suggests that bcc solid solutions may be most likely to conform to the MJS model. It is noted that bcc solid solutions are an important microstructural component in emerging Nb- and W-based alloys for high temperature applications for which creep performance is a critical concern.

Notable cases for which the MJS model will likely *not* be applicable include fcc metals and alloys. In these cases, dislocations are generally dissociated in a planar manner and do not exhibit a tendency for alignment along any particular line directions. Diamond cubic and zinc blende structures might also be suspected to deform *via* the jog dragging mechanism. Due to large Peierls valleys, both the screw and 60 degree orientations are prominent (slowest moving),

indicating that criteria (b) and (c) should be satisfied. However, materials, such as Si, Ge, and GaAs, tend to have only modest stacking fault energies, indicating that cross-slip should be relatively infrequent. Consequently, dislocation motion is likely to remain more planar, and superjogs are not expected to develop in sufficient density such that they control deformation.

VI. CONCLUSIONS

Jogged screw dislocations have been directly observed via TEM investigation of both $1/2\langle 110 \rangle$ dislocations in γ -TiAl and a-type $1/3\langle 11\bar{2}0 \rangle$ dislocations in the α phase of Ti-6242. The reason that these apparently dissimilar phases appear to deform via a similar dislocation mechanism are discussed. We have presented a modification of the original jogged-screw model to account for the fact that many of the jogs actually observed are quite tall (hundreds of Burgers vectors high), indicating that they have developed naturally as a result of multiple cross slip during creep deformation. Therefore, the MJS model incorporates a stress-dependent upper bound to the height of tall jogs that can be dragged. All jogs above this height are considered to act as sources. By incorporating these changes, the MJS model yields a natural stress dependence of about 5 at lower stresses, with larger values at high stresses. Excellent agreement is obtained between the MJS model and experimental data for γ -TiAl. The absolute creep rates predicted for Ti-6242 are larger than those found experimentally, which might be a result of the strong interaction between dislocations and silicide precipitates in this complex alloy. Finally, it is argued that the MJS model may also be applicable to creep of bcc solid-solution alloys based on the fact that the criteria for the formation of superjogs on screw dislocations should be satisfied for these alloys also.

REFERENCES

1. R.L. Coble: *J. Appl. Phys.*, 1963, vol. 34, pp. 1679-82.
2. F.R.N. Nabarro: *Report Conf. Strength of Solids (University of Bristol)*, Conf. Proc., 1948, pp. 75-90.
3. C. Herring: *J. Appl. Phys.*, 1950, vol. 21, pp. 437-45.
4. J. Harper and J.E. Dorn: *Acta Metall.*, 1957, vol. 5, pp. 654-65.
5. J.R. Weertman: *J. Appl. Phys.*, 1957, vol. 28, pp. 1185-89.
6. F.R.N. Nabarro: *Phil. Mag.*, 1967, vol. 16, pp. 231-37.
7. J.R. Weertman: *J. Appl. Phys.*, 1955, vol. 26, pp. 1213-17.
8. W.D. Nix and B. Ilshner: *5th Int. Conf. Strength of Metals and Alloys*, Conf. Proc., P. Haasen, V. Gerold, and G. Kostorz, eds., Pergamon Press, Oxford, United Kingdom 1979, pp. 1503-30.
9. H. Brehm and G. Daehn: *Metall. Mater. Trans. A*, 2002, vol. 33A, pp. 363-71.
10. G.B. Viswanathan, V.K. Vasudevan, and M.J. Mills: *Acta Mater.*, 1999, vol. 47, pp. 1399-1411.
11. C.R. Barrett and W.D. Nix: *Acta Metall.*, 1965, vol. 13, pp. 1247-58.
12. P.B. Hirsch and D.H. Warrington: *Phil. Mag.*, 1961, vol. 6, pp. 735-68.
13. N.F. Mott: *Creep and Fracture of Metals at High Temperatures*, Proc. NPL Symp., HMSO, London, 1956, pp. 21-24.
14. L. Raymond and J.E. Dorn: *Trans. AIME*, 1964, vol. 230, pp. 560-68.
15. J.P. Hirth and J. Lothe: *Theory of Dislocations*, 2nd ed., John Wiley & Sons, Inc., New York, NY, 1982.
16. A.K. Mukherjee, J.E. Bird, and J.E. Dorn: *Trans. Am. Soc. Met.*, 1969, vol. 62, pp. 155-79.
17. K. Xu and R.J. Arsenault: *Acta Mater.*, 1999, vol. 47, pp. 3023-40.
18. H. Siethoff, W. Schroter, and K. Ahlborn: *Acta Metall.*, 1985, vol. 33, pp. 443-48.
19. E. Furubayashi: *J. Phys. Soc. Jpn.*, 1969, vol. 27, pp. 130-46.
20. G.B. Viswanathan: Ph.D. Thesis, University of Cincinnati, Cincinnati, OH, 1997.
21. J. Beddoes, W. Wallace, and L. Zhao: *Int. Mater. Rev.*, 1995, vol. 40, pp. 197-217.
22. T.A. Parthasarathy, M.G. Mendiratta, and D.M. Dimiduk: *Scripta Mater.*, 1997, vol. 37, pp. 315-21.
23. W. Sprengel, H. Nakajima, and H. Oikawa: *Mater. Sci. Eng. A*, 1996, vol. A213, pp. 45-50.
24. J.N. Wang and T.G. Nieh: *Acta Mater.*, 1998, vol. 46, pp. 1887-1901.
25. B. Viguier, K.J. Hemker, J. Bonneville, F. Louchet, and J.L. Martin: *Phil. Mag. A*, 1995, vol. 71, pp. 1295-1313.
26. M. Lu and K.J. Hemker: *Acta Mater.*, 1997, vol. 45, pp. 3573-85.
27. Y. Ishikawa and H. Oikawa: *Mater. Trans., JIM (Jpn.)*, 1994, vol. 35, pp. 336-45.
28. S. Sriram, D.M. Dimiduk, P.M. Hazzledine, and V.K. Vasudevan: *Phil. Mag. A*, 1997, vol. 76, pp. 956-93.
29. F. Louchet and B. Viguier: *Phil. Mag. A*, 1995, vol. 71, pp. 1313-33.
30. G.B. Viswanathan and V.K. Vasudevan: *Gamma Titanium Aluminides*, TMS-AIME, 1995, pp. 967-74.
31. S. Kroll, H. Mehrer, N. Stolwijk, C. Herzig, R. Rosenkranz, and G. Frommeyer: *Z. Metallkd.*, 1992, vol. 83, pp. 591-95.
32. U. Messerschmidt, M. Bartsch, D. Haussler, M. Aindow, R. Hattenhauer, and I.P. Jones: *High-Temperature Ordered Intermetallic Alloys VI. Part I*, J.A. Horton, I. Baker, S. Hanada, R.D. Noebe, and D.S. Schwartz, eds., Materials Research Society, Pittsburgh, PA, 1995, vol. 364, pp. 47-52.
33. J.P. Simmons, M.J. Mills, and S.I. Rao: *High-Temperature Ordered Intermetallic Alloys VI. Part I*, J.A. Horton, I. Baker, S. Hanada, R.D. Noebe, and D.S. Schwartz, eds., Materials Research Society, Pittsburgh, PA, 1995, vol. 364, pp. 137-44.
34. S. Karthikeyan, G.B. Viswanathan, Y.-W. Kim, V.K. Vasudevan, and M.J. Mills: in *ISSI-3. 3rd Int. Conf. on Structural Intermetallics*, K.J. Hemker, D.M. Dimiduk, H. Clemens, R. Darolia, H. Inui, J.M. Larsen, V.K. Sikka, M. Thomas, and J.D. Whittenberger, eds., TMS, Warrendale, PA, 2001, pp. 717-23.
35. S. Karthikeyan, G.B. Viswanathan, Y.-W. Kim, P.I. Gouma, V.K. Vasudevan, and M.J. Mills: *Mater. Sci. Eng. A*, 2001, in press.
36. P.J. Bania and J.A. Hall: *Titanium Science and Technology*, Deutsche Gesellschaft fur Metallkunde, Oberursel, Germany, 1985, pp. 2371-78.
37. S. Ranganath and R.S. Mishra: *Acta Mater.*, 1996, vol. 44, pp. 927-35.
38. G.B. Viswanathan, R.W. Hayes, and M.J. Mills: unpublished research, 2001.
39. M. Koppers, C. Herzig, M. Friesel, and Y. Mishin: *Acta Mater.*, 1997, vol. 45, pp. 4181-91.
40. A. Gershick, D.G. Pettifor, and V. Vitek: *Phil. Mag. A*, 1998, vol. 77, pp. 999-1012.
41. T. Neeraj, D.H. Hou, G.S. Daehn, and M.J. Mills: *Acta Mater.*, 2000, vol. 48, pp. 1225-38.
42. S. Ikeno and E. Furubayashi: *Phys. Status Solidi A*, 1975, vol. 27, pp. 581-90.
43. V. Vitek: *Cryst. Lattice Defects*, 1974, vol. 5, pp. 1-34.
44. S. Ikeno and E. Furubayashi: *Phys. Status Solidi A*, 1972, vol. 12, pp. 611-22.
45. S. Ikeno: *Phys. Status Solidi A*, 1976, vol. 36, pp. 317-28.
46. J.R. Low, Jr. and A.M. Turkalo: *Acta Metall.*, 1962, vol. 10, pp. 215-27.